Magnetotransport and domain structures in nanoscale NiFe/Cu/Co spin valve

L. Kong[a)]
NanoStructure Laboratory, Department of Electrical Engineering, Princeton University, Princeton, New Jersey 08544

Q. Pan
Department of Electrical Engineering, University of Minnesota, Minneapolis, Minnesota 55455

B. Cui, M. Li, and S. Y. Chou
NanoStructure Laboratory, Department of Electrical Engineering, Princeton University, Princeton, New Jersey 08544

Nanoscale spin-valve structures with a width as small as 70 nm were fabricated using nanoimprint lithography and ion milling or lift off. The spin-valve multilayers consisting of NiFe(10 nm)/Co(1 nm)/Cu(13 nm)/Co(10 nm)/NiFe(2 nm) were deposited using direct current sputtering. The effects of device size, as well as fabrication process on domain structures, switching fields, switching field variation, and giant magnetoresistive ratio were investigated using scanning electron microscopy, atomic force microscopy, magnetic force microscopy, and magnetoresistance measurements. © *1999 American Institute of Physics.* [S0021-8979(99)63508-3]

I. INTRODUCTION

Nanoscale spin-valve structures are important not only for practical applications but also for fundamental understanding of micromagnetics. Simulations indicate that the magnetization reversal process in a spin valve differs when its size shrinks to submicron.[1] As shown in a spin-valve cell with a 0.15 μm width,[2] a pinned layer used in a conventional spin valve may not be necessary, since each submicron layer could become spontaneously magnetized (e.g., single domain). In this article, we report on fabrication of the magnetic multilayer NiFe/Cu/Co with 70 nm width using nanoimprint lithography and an ion-milling or lift-off process, and the magnetotransport behavior, domain structures, and switching fields of the devices.

II. FABRICATION

Two processes were used to fabricate the nanoscale spin valves with a magnetic multilayer of NiFe(10 nm)/Co(1 nm)/Cu(13 nm)/Co(10 nm)/NiFe(2 nm). One was subtractive, involving deposition, lithography, and ion milling. The other was additive, involving lithography, deposition and lift off. In the first method, the magnetic multilayer was first deposited on a SiO_2 substrate using direct current (dc) sputtering. Then nanoimprint lithography created a polymethyl methacrylate (PMMA) template on the magnetic multilayer,[3–5] followed by deposition of SiO_2 and a lift off. The SiO_2 structures served as a mask for ion milling of the spin-valve structures in the metal layer. After ion milling, the SiO_2 mask was removed and the final contacts were made.

In the second method, PMMA was first coated on a SiO_2 substrate and patterned using nanoimprint lithography. Then the magnetic multilayer was deposited on PMMA using dc sputtering. A lift off of PMMA left the spin-valve structures on the substrate.

A scanning electron microscopy (SEM) image of a typical magnetic multilayer pattern by ion milling is shown in Fig. 1. Figure 2 shows the atomic force microscopy (AFM) image of a bar with four leads patterned by ion milling. Both SEM and AFM observations indicate that the edge of the lift-off patterns is not as smooth as that of the ion-milling patterns.

III. RESULTS AND DISCUSSION

The magnetotransport behavior and domain structures of the spin-valve structures were characterized using magnetoresistance measurements and magnetic force microscopy (MFM) measurements. It was found that the behavior was strongly affected by the pattern size and fabrication methods. The magnetoresistance (MR) measurements were carried out using a four-terminal technique and the external magnetic field was applied along the bar length in the plane of the film, as shown in Fig. 2. The magnetization states of the patterned

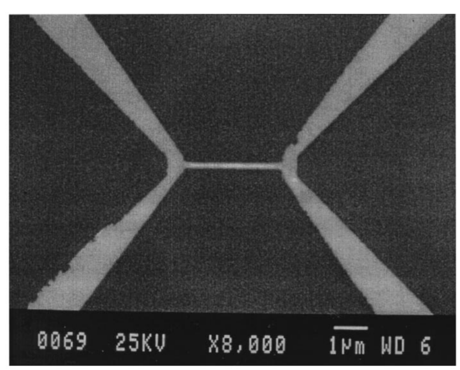

FIG. 1. SEM image of patterned spin-valve bar of 100 nm×3 μm with four leads fabricated by ion milling.

[a)]Electronic mail: lkong@ee.princeton.edu

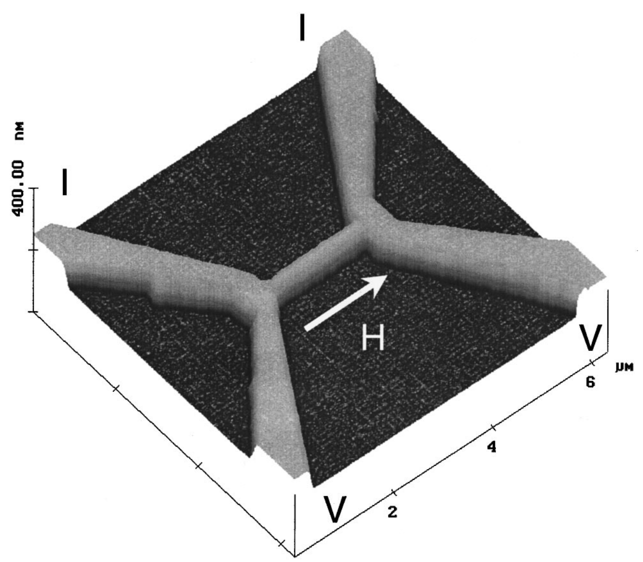

FIG. 2. AFM image of patterned spin-valve bar of 150 nm×2 μm with four leads and the schematic of MR measurements.

magnetic multilayers were observed using a commercial MFM with a high-resolution tip made in-house.

First, we will discuss the experimental results of the magnetic patterns fabricated using ion milling. Figure 3 is a typical giant magnetoresistive (GMR) curve for the patterned spin-valve bar of 300 nm×3 μm. As the magnetic field increases, the steep jump in the GMR curve corresponds to the switching field (H_{s1}) of the soft magnetic layer, NiFe(10 nm)/Co(1 nm). This layer is primarily a magnetic soft alloy, NiFe. As the magnetic field continuously increases, the sudden drop in the GMR curve corresponds to the switching field (H_{s2}) of the hard magnetic layer, which has Co(10 nm)/NiFe(2 nm). The patterned bar has a smaller resistance when the magnetic soft and hard layers are aligned in the same direction, and has a larger resistance when the two layers point in the opposite magnetic direction.

If the maximum sweep field is less than the switching field of hard layer but larger than that of soft layer, a minor loop of MR curve will be achieved. Figure 4(a) is the GMR curve of the pattern of 200 nm×3 μm. The switching field is around 325 Oe for hard layer and around 100 Oe for soft layer, respectively. Figure 4(b) shows a minor loop of magnetoresistance when the magnetic field was sweeped between +170 Oe and −170 Oe. In Fig. 4(b), only the soft layer was switched and the hard layer remained in the same direction when the magnetic field was applied to the sample. This further confirms the above analysis, revealing that GMR curves can be correlated with magnetization reversal process. It is apparent that the GMR effect in nanoscale magnetic patterns is very helpful for understanding micromagnetics.

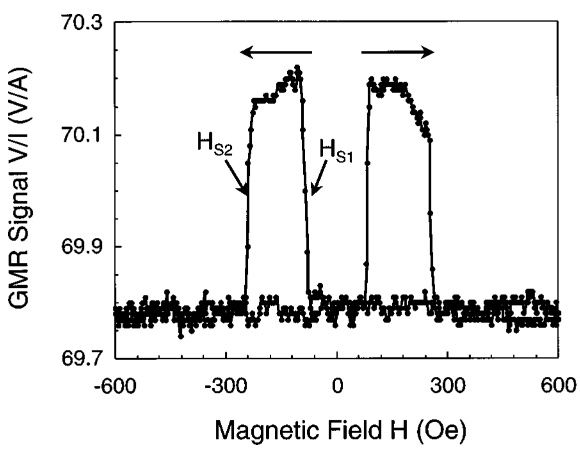

FIG. 3. GMR curve of patterned spin-valve bar of 300 nm×3 μm, where H_{s1} = 85 Oe and H_{s2} = 240 Oe. The pattern was fabricated by ion milling.

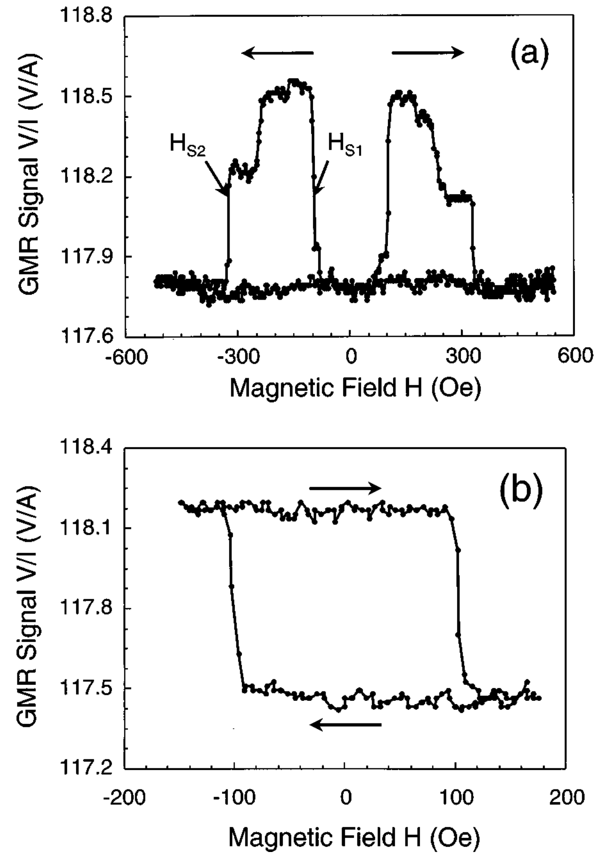

FIG. 4. (a) GMR curve and (b) minor loop of patterned spin-valve bar of 200 nm×3 μm by ion milling. In Fig. (a), H_{s1} = 100 Oe and H_{s2} = 325 Oe.

In order to observe clearly the domain structures using MFM, the patterned magnetic multilayer bars without magnetic leads were fabricated. Figure 5 shows an example of an MFM image for patterned a spin-valve bar of 150 nm×2 μm. The two opposite magnetic poles at the bar ends suggest that the magnetic multilayer bar form a single domain. From the MFM observations, it is found that the multilayer bars are single domain when the bar width is less than 200 nm.

The average switching fields in spin-valve structures with 2 μm length as a function of the bar width are given in Fig. 6. It can be seen that with the reduction of the bar width, the switching field (H_{s2}) of the hard layer has a significant increase at the width around 200 nm, while the switching field (H_{s1}) of the soft layer only increases slightly. The significant increase of H_{s2} at 200 nm width suggests that the mechanism of switching for pattern width larger than 200 nm

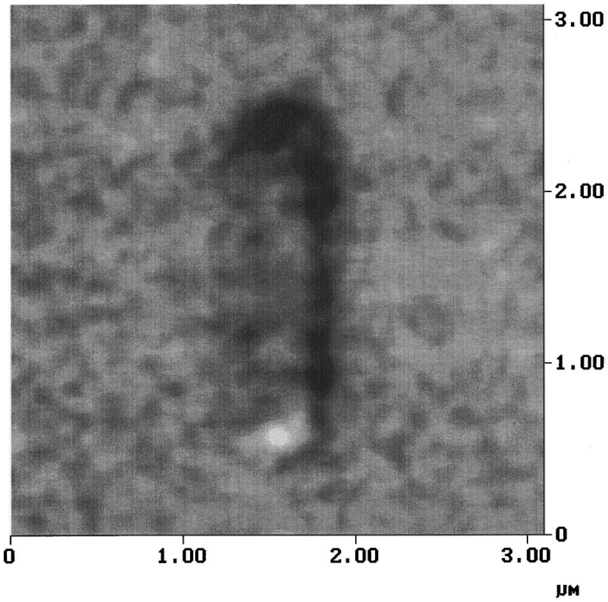

FIG. 5. MFM image of patterned spin-valve bar of 150 nm×2 μm without leads by ion milling. Two opposite magnetic poles at bar ends indicate the formation of single domain.

could be different from that for width less than 200 nm.

Moreover, it is found that the GMR ratio also depends on the device size. For a thin film sample, the GMR ratio is nearly 1%. But for the 400, 150, and 70 nm-wide patterns, the ratios are 0.72%, 0.65% and 0.47%, respectively. The decrease in the GMR ratio might be caused by two reasons. One is that the electron scattering at the pattern edge plays a greater role in the electron transport when the pattern becomes narrow. The other is that the ion-milling process can affect the transport behavior at the edges of a pattern, which becomes significant in the narrow pattern.

When the MR measurement of the spin-valve structures was repeated at different times, the switching field of the same structure was observed to be varied. The narrower the pattern, the larger the variation of switching field. The variation of switching field can be as large as 15%. This is believed to be related to the incoherent switching (e.g., reversal

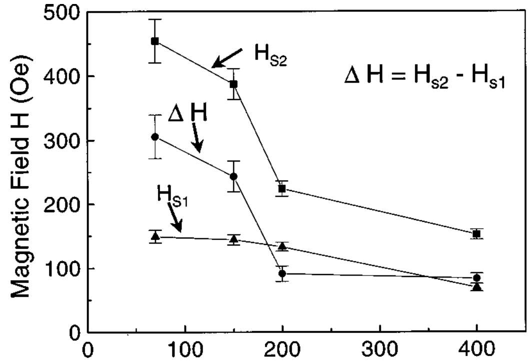

FIG. 6. Switching fields as a function of bar width. The patterned bars are 2 μm long and were made by ion milling.

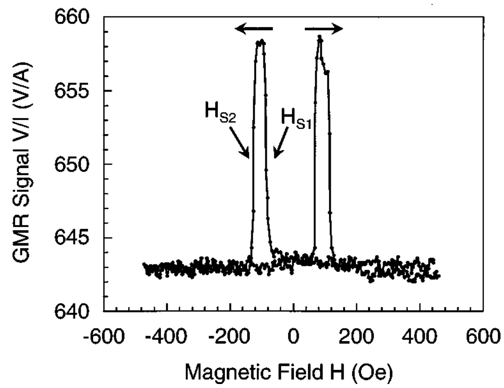

FIG. 7. GMR curve of spin-valve bar patterned by lift-off process. The bar size is 100 nm×3 μm. In the figure, $H_{s1}=85$ Oe and $H_{s2}=125$ Oe.

nucleation and magnetization distortion). The different switching fields correspond to different energy barrier of nucleation.[6] Simulations also show that the different domain configuration at the ends of patterned magnetic film leads to the variation of switching field.[7] In our case, the magnetic leads make the switching process even more complicated.

The spin-valve bar fabricated using lift-off process has a switching field significantly lower than that of ion-milling pattern. As shown in Fig. 7, the switching fields of a pattern of 100 nm×3 μm were around 125 Oe for the hard layer and around 85 Oe for the soft layer. For the pattern with the same aspect ratio fabricated by ion milling, the switching fields were around 450 Oe for the hard layer and around 150 Oe for the soft layer. The significantly reduction of switching field in the lift-off structures may be caused by edge roughness, as confirmed by SEM inspection.

IV. CONCLUSIONS

We have fabricated and characterized spin-valve structures consisting of NiFe(10 nm)/Co(1 nm)/Cu(13 nm)/Co(10 nm)/NiFe(2 nm) with size down to 70 nm×1 μm. When the multilayer bar width was less than 200 nm, the formation of single domain was found. As the pattern width decreased, the switching fields for both the hard layer and the soft layer increased. The fluctuation of switching field in the spin-valve structures was observed. The ion-milling patterning affected significantly the GMR ratio of narrower magnetic patterns. The spin valve patterned by lift off had a much smaller switching field than that patterned by ion milling, which may be caused by edge roughness.

ACKNOWLEDGMENT

This work was supported in part by DARPA and ONR.

[1] Y. Zheng and J.-G. Zhu, IEEE Trans. Magn. **32**, 4237 (1996).
[2] B. A. Everitt, A. V. Pohm, and J. M. Daughton, IEEE Trans. Magn. **34**, 1060 (1998).
[3] S. Y. Chou, P. R. Krauss, and P. J. Renstrom, Science **272**, 85 (1996).
[4] S. Y. Chou and P. R. Krauss, *Micro- and Nano- Engineering International Conference, Glasgow, Scotland, United Kingdom*, (1996).
[5] S. Y. Chou, P. R. Krauss, and P. J. Renstrom, Appl. Phys. Lett. **67**, 3113 (1995).
[6] W. Wernsdorfer, B. Doudin, D. Mailly, K. Hasselbach, A. Benoit, J. Meier, J.-Ph. Ansermet, and B. Barbara, Phys. Rev. Lett. **77**, 1873 (1996).
[7] Y. Zheng and J.-G. Zhu, J. Appl. Phys. **81**, 5471 (1997).